Open access

https://jrisetgeotam.lipi.go.id/index.php/jrisgeotam

RISET
Geologi dan Pertambangan
Geology and Mining Research

Riset Geologi dan Pertambangan (2023) Vol.33, No.1, 1–15, DOI: 10.55981/risetgeotam.2023.1054

Research articles

Petrology, geochemistry and K-Ar dating of metamorphic rock in Ciletuh Mélange Complex, West Java, Indonesia

Rinaldi Ikhram[1], Ildrem Syafri[2], Mega F. Rosana[2]

[1]Faculty of International Resource Science, Akita University, Akita, Japan
[2]Faculty of Geological Engineering, Padjadjaran University, Bandung, Indonesia

Keywords:
Ciletuh,
Metamorphic,
Petrology,
Geochemistry,
K-Ar Dating

Corresponding author:
Rinaldi Ikhram
Email address: rinaldikhram@gmail.com

Article history
Received: 25 June 2019
Revision: 14 January 2022
Accepted: 23 November 2022

ABSTRACT

The Ciletuh Mélange Complex in West Java, Indonesia, provides evidence of early Cenozoic subduction. This study aims to investigate the stratigraphic position, geological structure, metamorphic facies, and protoliths of the metamorphic rock units. The research methods employed geological mapping, petrology, and geochemical analysis. The samples collected exhibit different facies, including zeolites, greenschist, and epidote amphibolite. Protoliths consist of metasedimentary rocks such as metapellites, metapsammitics, meta-calcilates, and ortho-metamorphs such as metagabbro and metabasalt. Retrograde metamorphism, indicated by epidote, chlorite, and calcite in amphibolite schists, suggests lower temperature stress conditions. Hydrothermal changes are evidenced by some samples' occurrence of quartz and calcite veins. Geochemical analysis reveals that the provenance of metasedimentary rocks originated from a volcanic arc, while the metabasalt rock originated from an island arc tectonic environment. K-Ar dating indicates an age range of 55.2 - 37.8 million years ago, corresponding to the Early to Late Eocene. These metamorphic rocks are believed to have formed through regional metamorphism due to island arc subduction and the formation of accretionary prisms. Retrograde metamorphism signifies uplift or accretion processes after tectonic activity.

INTRODUCTION

The Ciletuh area in West Java, Indonesia, is known for its complex geological phenomena. This mélange complex exhibits unique features, including ophiolite and pre-Tertiary metamorphic rocks. Previous studies have classified the rock complexes into three pre-Tertiary units: Sekis Pasir Luhur, Gunung Beas Ultramafic Rocks, and Citirem Formation. The rock outcrops in the area are characterized as chaotic and mixed mélange, composed of ultramafic, metamorphic, deep-sea sediment, and continental sediment rocks (Sukamto, et., al., 1975; Thayyib et al., 1977; Sartono and Murwanto, 1987). These rocks are found as various-sized blocks enclosed within a weathered shale matrix (scaly clay), with each block having a faulted contact (Thayyib et al., 1977).

The variety of metamorphic rocks within the Melangè Ciletuh complex was first reported in detail by Thayyib et al. (1977) in their report on the status of the Melangè complex. Variations of greenschist and phyllite can be found in the Pasir Luhur and Gunung Badak areas (Suparka, 1995; Dirk, 1997; Prasetyo, 2016; Ikhram, 2019). In the vicinity of the Koneng Hideung area, there are outcrops of hard, fine to medium-grained white quartzite, which are also found in the Citisuk River with quartz veins, while Gunung Badak displays well-foliated dark gray phyllite. However, the reported occurrence of blueschist/glaucophane schist in Ciletuh, as mentioned by Thayyib et al. (1977), could not be proven by subsequent researchers (Satyana, 2021).

In the subsequent mapping conducted by Ikhram (2019), it was confirmed that metamorphic rocks are scattered randomly and separately in various locations, but there are also continuous occurrences along river channels. The identified types of metamorphic rocks include greenschist, phyllite, amphibolite schist, and quartzite. Metamorphic rock outcrops are typically found on the walls and riverbed. The metamorphic rocks are prominently exposed in the Citisuk River, Cibatununggul River, and numerous other river channels within the local area. There is no evidence of metamorphic rocks with a higher degree of metamorphism than amphibolite, such as ultra-high pressure, ultra-high temperature, and ultra-high pressure temperature.

However, detailed information on metamorphic rocks in Ciletuh is limited. This paper aims to provide a comprehensive analysis of the metamorphic rocks in Ciletuh, focusing on their variations, degree of metamorphism, protoliths, geochemistry, and geochronology using whole rock K-Ar dating.

METHODS

Detailed geological mapping at a scale of 1:10,000 has been conducted, which includes sample collection, recording the locations of rock outcrops, foliation direction, and other structures. Petrographic analysis was performed using a polarizing microscope. Thin sections were made at the Mineralogy and Petrology Laboratory of Padjadjaran University for 68 samples comprising amphibolite schist, greenschist, and phyllite. Whole rock geochemistry, including major elements, trace elements, and rare earth elements, was acquired at the INTERTEK Laboratory, Jakarta, by utilizing XRF (X-Ray Fluorescence) and ICP-MS (Inductively Coupled Plasma Mass Spectrometry) encompassing a total of seven muscovite-chlorite schist samples and three albite-epidote schist samples. This geochemical analysis will provide information about rock types, magma types, and estimates of the tectonic environment in which the rocks formed. For the metamorphic rock samples (greenschist), geochemical analysis is used to identify protoliths and interpret the tectonic environment and origin of the metasedimentary rocks. K-Ar dating was conducted by ActLabs (Activation Laboratories Ltd.) Canada on three whole rock samples of chlorite-muscovite-schists.

RESULT AND DISCUSSION

Occurrence of Metamorphic Rocks and Their Deformation Features

The Cikopo River presents an extensive distribution of metamorphic rocks exhibiting a well-defined wavy foliation structure. These metamorphic units are in juxtaposition with serpentinite rocks along the northern and southern banks of the river. In the Citisuk River, the metamorphic rocks display a prominent foliation characterized by the presence of green minerals such as chlorite and epidote, as well as mica, quartz, and plagioclase. Notably, foliation orientation changes were observed from the southeast-northwest trend to the southwest-northeast. Conversely, the Cikarikil River exposes gray-colored rocks that exhibit distinct foliation planes, often accompanied by abundant quartzite lenses. These rocks have undergone considerable weathering, leading to the development of a foliation direction from north-south to northeast-southwest. Mineral assemblages observed within these rocks include quartz, muscovite, and chlorite. The geological attributes observed in all three rivers encompass significant structural

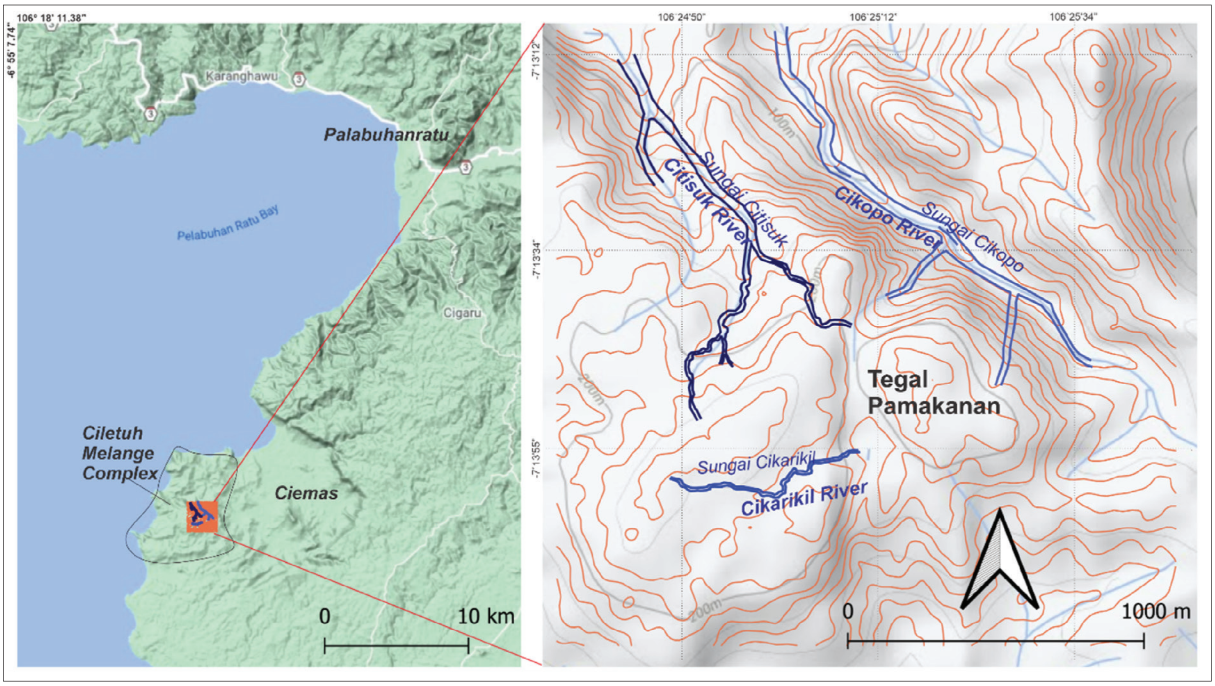

Figure 1. Location Index of Research Area (Gunung Beas Block) marked by a red square boundary, the research focus is on the Citisuk River, Cikopo River, and Cikarikil River along with several tributaries.

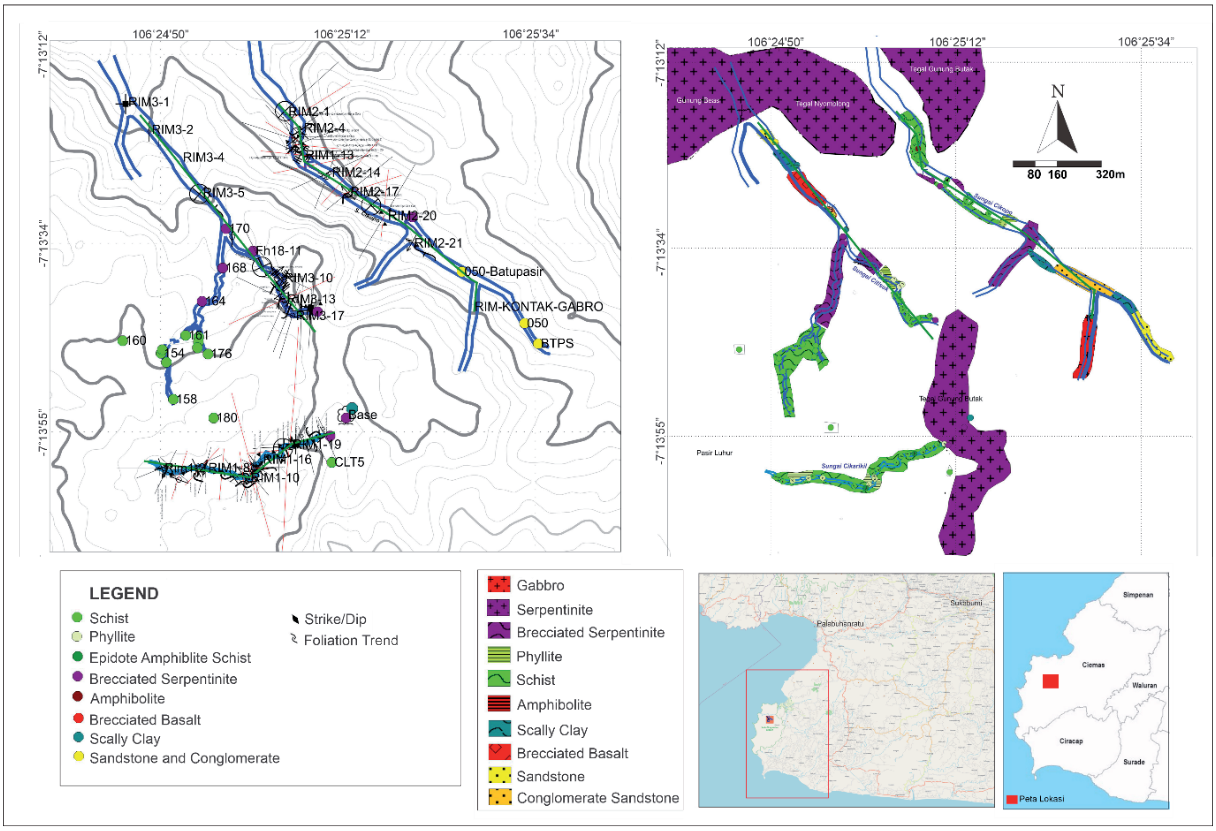

Figure 2. Location map of sample collection and its lithological boundaries

complexities, including contacts with diverse lithologies and fault systems. Several places show that fault contacts with serpentinite interrupt the distribution of metamorphic rocks. Similar discoveries are found in the river's southern section, where a distinct contact between metamorphic rocks and brecciated serpentinite exists. The serpentinite body is structurally emplaced on an overlying position relative to the schist, exhibiting an orientation of N 360ºE / 30º. Some locations also reveal exposed serpentinite with foliation. In the southern part, exposures of scaly clay exhibit signs of weathering structures, characterized by weathering lines in all planes with a dominant orientation of N 115º E / 35º (Figure 3-D). Additionally, amphibolite exposures with gneissic structures consisting of hornblende and plagioclase (Figure 3-B) are found in this river. Based on the measurements of joint sets, three dominant directions were identified: N 90º-130ºE, N 20º-40ºE, and N 160º-170ºE, representing two stress regimes: north-south extension and northeast-southeast compression.

From the fault analysis, it can be concluded that various fault types are present, including reverse faults and horizontal faults with northwest-southeast and northeast-southwest orientations. Based on the rose diagram of foliation orientations, it is evident that metamorphic rocks in the three rivers exhibit three dominant orientations: N 355º E, N 340º E (northwest-southeast), and N 250º E (northeast-southwest). Geological cross-sections indicate that these orientations give rise to predominantly northward-dipping anticlines and synclines.

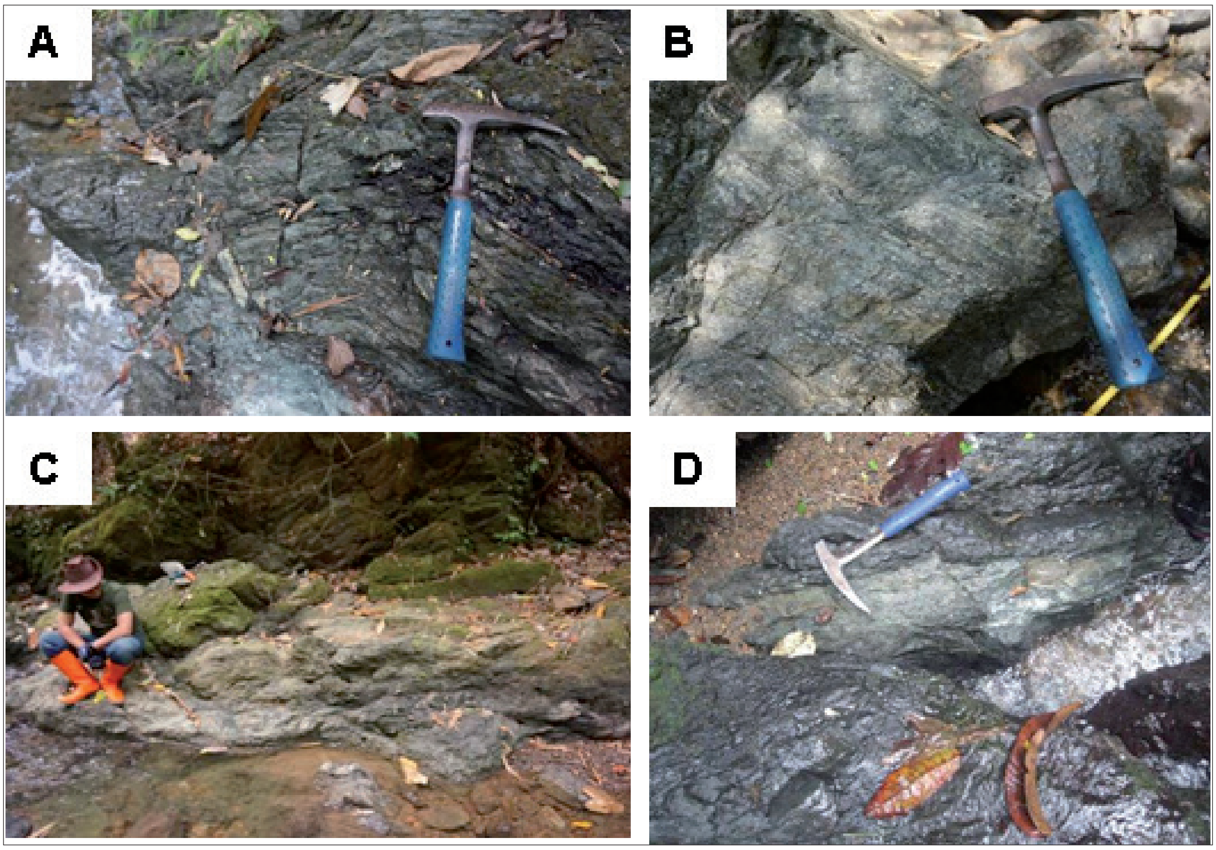

Figure 3. (A) Outcrop of green schist with foliation in Citisuk River, (B) Amphibolite schist in Cikopo River, (C) Outcrop of epidote schist in Cikopo River; (D) Amphibolite schist embedded in scaly clay.

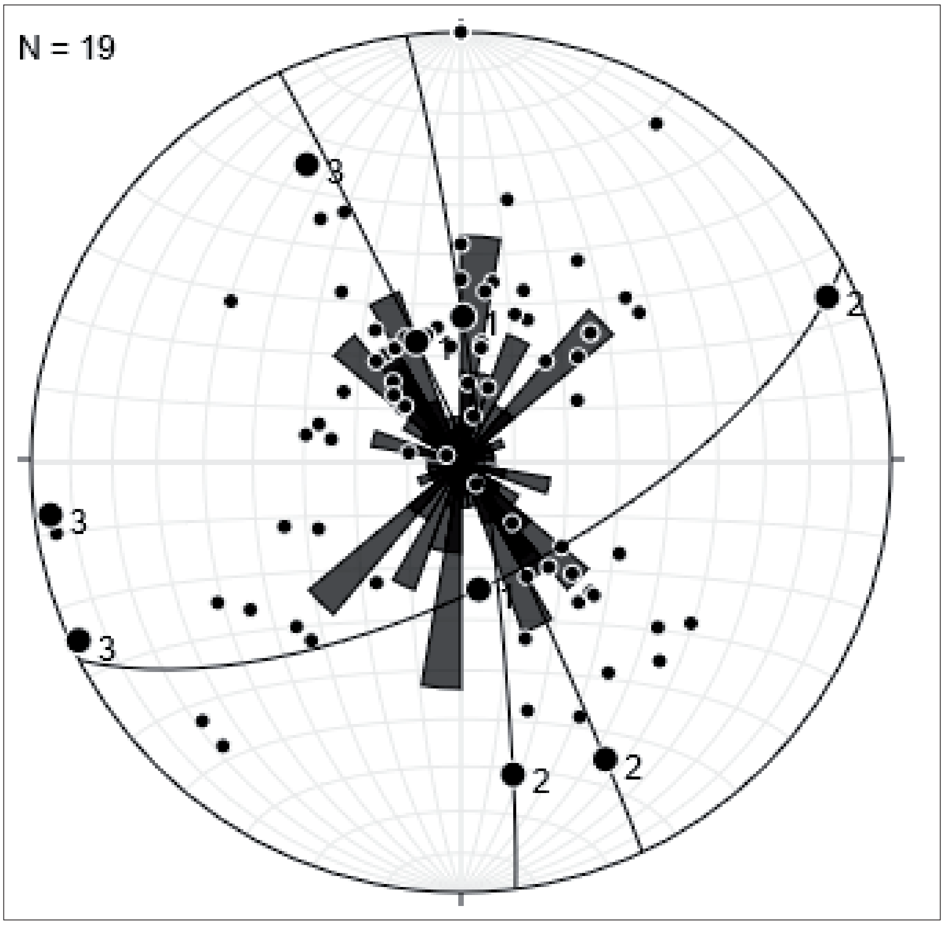

Figure 4. Rosette Diagram showing the orientation of foliation in metamorphic rocks in the Ciletuh area.

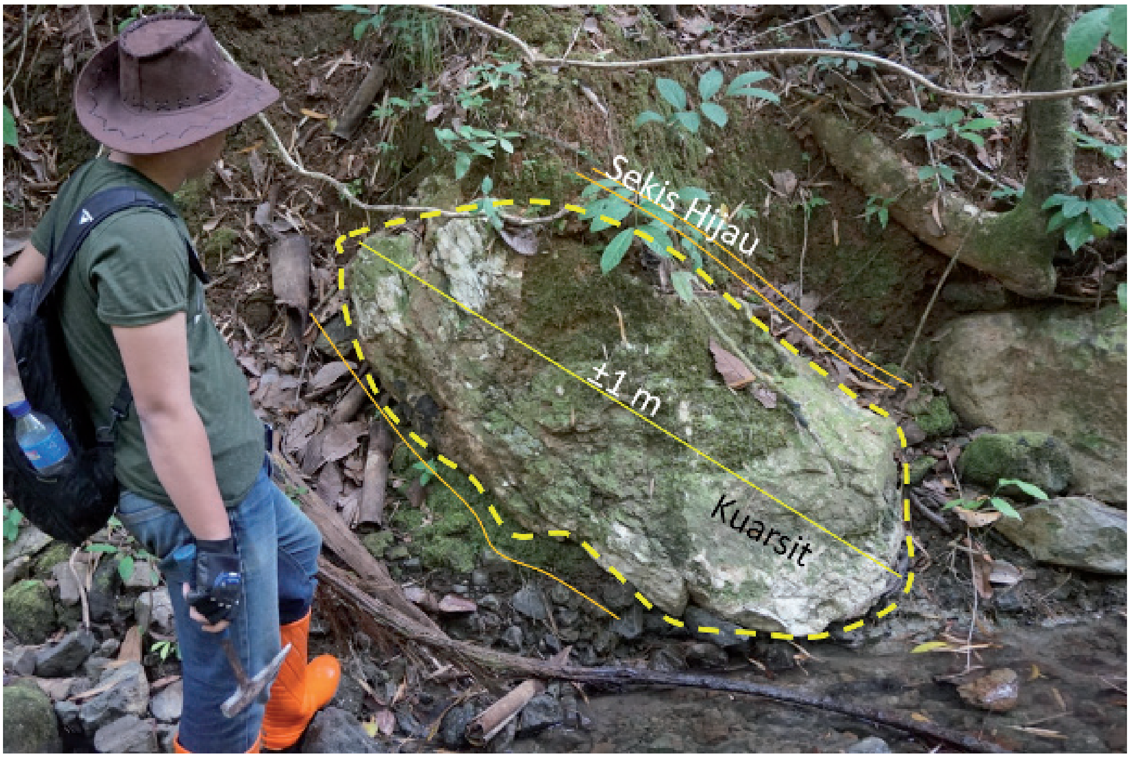

Figure 5. Quartzite lenses within greenschist foliation with up to 1 meter elongation.

Petrographic Description

Thin rock sections were prepared from samples collected at the Citisuk River and Tegal Pamakanan River. The selected samples (RIM 3-1, RIM 3-10, RIM 3-17, RIM 2-18, RIM 1-18, and RIM 1-10) were analyzed for mineral compositions (Table 1) and classified in Figure 6. Sample RIM 3-10 exhibited two distinct mineralogical domains: one rich in phyllosilicates (white mica and chlorite) and the other rich in quartz and feldspar. Some samples showed separation between phyllosilicate and quartz/feldspar layers. In the phyllosilicate-rich domain, fibrous chlorite accompanied fine-grained white mica. Quartz grains aligned with foliation, while larger quartz grains lacked the preferred orientation and were surrounded by elongated chlorite. Partially degraded samples showed different mineral compositions, including quartz + feldspar + white mica + chlorite and white mica + chlorite domains. Detailed mineral compositions can be found in Table 1, and Figure 6 provides the classification plot.

Table 1. Mineralogy of greenschist and amphibolite in Ciletuh.

Location	**Contituent Minerals**									**Rock Name**	**Facies**	**Protolith**
	Qz	Pl	Chl	Ep	Hb	Ca	Ms	Gp	Op			
RIM 3-1	●	▲	●	■	▲	-	▲	-	▲	Epidote chlorite schist	Epidote Amphibolite	Wacke or volcaniclastic
RIM 3-10	●	■	●	▲	-		●	-	▲	Muscovite chlorite schist	Greenschist	Pelitic
RIM 3-17	■	●	●	■	-	■	-	-	▲	Epidote chlorite schist	Greenschist	Basaltic or volcaniclastic
RIM 2-18	●	■	▲	▲	-	●	■	▲	▲	Chlorite muscovite schist	Greenschist	Pelitic
RIM 1-18	●	▲	■	▲	-	-	●	-	▲	Chlorite muscovite schist	Greenschist	Pelitic
RIM 2-8	■	●	■	▲	●	▲	-	-	▲	Epidote-hornblende Schist	Amphibolite	Basaltic

Explanation: Qz = Quartz, Pl = Plagioclase, Chl = Chlorite, Ep = Epidote, Hb = Hornblende, Ca = Calcite, Ms = Muscovite, Gp = Graphite, Op = Opaque; (●)=Abundant, (■)=Medium, (▲) Rare, (-) = None

Sample RIM 3-1 displayed a poikiloblastic texture with inclusions within the porphyroblast. It contained quartz, plagioclase, chlorite, calcite, and epidote. The plagioclase showed significant alteration, forming carbonate and epidote within the crystal. Muscovite exhibited foliation, while chlorite displayed a fibrous texture. Interlocking quartz lenses were also observed. The presence of muscovite and chlorite indicated lower-greenschist facies.The greenschist's protolith originated from various rock types, including mudstones, sandstones, carbonate-bearing sandstones, and basaltic rocks. The muscovite-rich schist resulted from the transformation of K and Al constituents from clay minerals to muscovite during metamorphism, especially in mudstones. Epidote-rich schist was associated with Mg enrichment in Ca-bearing minerals like Ca-plagioclase during metamorphism, potentially sourced from sandstones, calcarenites, and/or basaltic rocks.

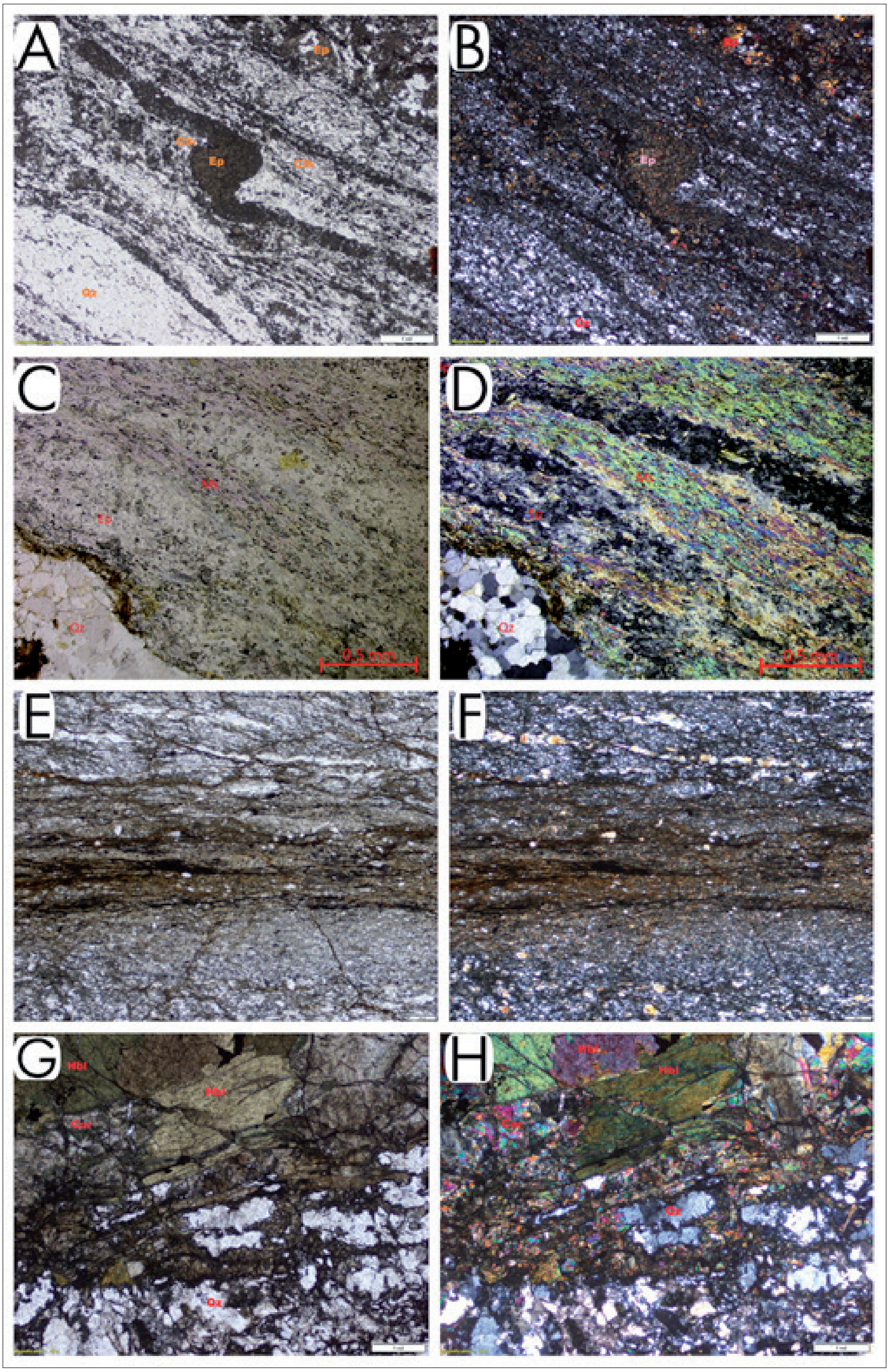

Figure 6. Microscopic features of samples: (A) & (B) RIM 3-1 sample, parallel polarization and crossed polarization of epidote-chlorite schist; (C) & (D) RIM 3-10 sample, parallel polarization and crossed polarization of muscovite-chlorite schist; (E) & (F) RIM) RIM 1-2 sample, parallel polarization and crossed polarization of muscovite-graphite phyllite; (G) & (H) RIM 2-8 sample, parallel polarization and crossed polarization of amphibolite

Phyllites were collected from the Cikarikil River site at stations RIM 1-2 and RIM 1-12. RIM 1-2 represented Talc Muscovite Phyllite with quartz, talc, muscovite, and graphite domains. The foliation was not well-developed due to the random orientation of minerals. RIM 1-12 represented Chlorite Epidote Phyllite with quartz, plagioclase, and unidentified clay minerals. Limited occurrence of metamorphic minerals indicated low-grade metamorphism.

Amphibolites were found in sections RIM 2-8 and RIM 3-4. They exhibited distinct domain variations, including quartz-feldspar layers and amphibole layers. The mineral composition included plagioclase, hornblende, epidote, and chlorite. Plagioclase altered into epidote, and tremolite-actinolite formed at the boundaries due to metamorphism. Chlorite was present at the hornblende rim, and plagioclase was altered to calcite. Altered minerals such as epidote and chlorite were common in amphibolite sections.

Whole Rock Geochemistry

Based on the XRF and ICP-MS results, the green amphibolite samples exhibit distinct chemical characteristics regarding of major elements and trace elements. The SiO_2 content in RIM 2 and RIM 3-16 samples from the Cikopo River is relatively low, ranging from 40.95% to 50.52%. However, in RIM 1-18, RIM 3-10A, and RIM 3-13 samples from the Cikarikil and Citisuk Rivers, the SiO_2 content is relatively high, ranging from 59.57% to 60.12%. Similar patterns are observed for the K_2O content, where the RIM 2 and RIM 3-16/17 samples from the Cikarikil River have lower K2O content (0.11% to 0.44%) than to other samples with K_2O content above 2%.

Table 2. Composition of major elements in representatite samples of metamorphic rocks.

Sample / Elemen	RIM 3-10A (MPL)	RIM 3-13 (MPL)	RIM 1-18 (MPL)	RIM 3-16 (MB)	RIM 3-17 (MB)/ (MPS)	RIM 2B (MB)/ (MPS)	RIM 1-10 (MB)	RIM 2-10 (MB)	RIM 2G (MB)/ (MPS)	RIM 2M (MB)/ (MPS)
Major Element (wt%)										
Al_2O_3	17.41	16.97	17.24	17.35	16.24	14.30	13.93	13.68	13.07	14.13
CaO	2.97	2.66	2.96	11.19	7.19	8.04	14.00	14.39	10.86	13.57
Cr_2O_3	0.19	0.13	0.02	0.05	0.26	0.07	0.06	0.07	0.06	0.05
Fe_2O_3	7.44	7.35	7.49	9.90	6.09	10.07	8.54	8.30	8.78	9.38
FeO	6.69	6.61	6.74	8.91	5.48	9.06	7.68	7.47	7.90	8.44
K_2O	4.44	2.91	2.78	0.07	0.44	0.11	0.24	0.23	0.11	0.33
MgO	2.57	2.86	2.80	3.62	4.83	7.97	5.29	5.09	6.39	5.83
MnO	0.12	0.18	0.16	0.21	0.11	0.17	0.18	0.18	0.15	0.18
Na_2O	0.79	2.86	2.64	2.61	3.84	4.25	3.19	3.19	3.91	2.30
P_2O_5	0.150	0.162	0.153	0.234	0.073	0.279	0.092	0.089	0.211	0.130
SiO_2	60.12	59.57	59.48	50.52	58.71	47.61	40.96	40.95	48.23	44.86
TiO_2	0.84	0.81	0.82	1.07	0.47	1.75	0.95	0.93	1.38	1.23
S	0.393	0.060	0.141	<0.002	<0.002	0.170	<0.002	<0.002	0.083	<0.002
LOI	3.06	3.70	2.69	2.80	2.05	5.68	12.85	13.15	7.21	7.47
Total	100	100	99.4	99.6	100	100	100	100	100	99.5

The Al_2O_3 content in the RIM 2 samples is relatively low, ranging from 13.07% to 14.30%, compared to other samples with Al_2O_3 content ranging from 16.24% to 17.41%. The CaO content in the RIM 2 and RIM 3-17 samples (10.86% to 14.39%) is significantly higher than other samples. Similar trends are observed for the MgO and Fe_2O_3 contents, where the RIM 2 and RIM 3-17 samples show higher values than others. The CaO content is notably significant in the RIM 2C/2D samples, ranging from 14.00% to 14.39%. The Fe_2O_3 content does not show significant differences among the samples, ranging from 6.61% to 9.06%.

The samples RIM 3-10A, RIM 3-13, and RIM 1-18 exhibit relatively low concentrations of elements Al, K, Ba, Bi, Rb, Th, Tl, and Ce, compared to the other samples, namely RIM 2, RIM 3-16, and RIM 17, which show relatively high concentrations of these elements. Conversely, the concentrations of Ca, Cr, Mg, and Na in the RIM 2, RIM 3-16, and RIM 17 samples are relatively higher compared to the RIM 3-10A, RIM 3-13, and RIM 1-18 samples. A significant Ca content is observed in the RIM 2C/2D sample. The Fe content does not show significant differences among the samples.

Based on the observed differences in major and trace element concentrations, variations in the protoliths of metamorphic rocks in Ciletuh can be inferred. Samples with high SiO_2, Al_2O_3, K_2O, Al, K, Ba, Bi, Rb, Th, Tl, and Ce are likely derived from metapelitic protoliths, indicated by the presence of quartz and muscovite/sericite minerals. Conversely, samples rich in CaO, MgO, Fe_2O_3, Ca, Cr, Mg, and Na are suspected to originate from metapsammite or meta-graywacke protoliths, as indicated by the presence of plagioclase, chlorite, epidote, quartz, and calcite minerals.

Analysis of the SiO_2 vs. major element comparison diagram (Figure 7) reveals significant differences between specific samples (RIM 3-10A, RIM 3-13, RIM 3-17, and RIM 1-18) and others. The relationships between SiO_2 and CaO, and SiO_2 and MgO appear to be inverse, while SiO_2 shows a direct correlation with Al_2O_3 and P_2O_5. The relationship between SiO_2 and K_2O remains relatively consistent, except for the samples as mentioned above, which exhibit a direct correlation.

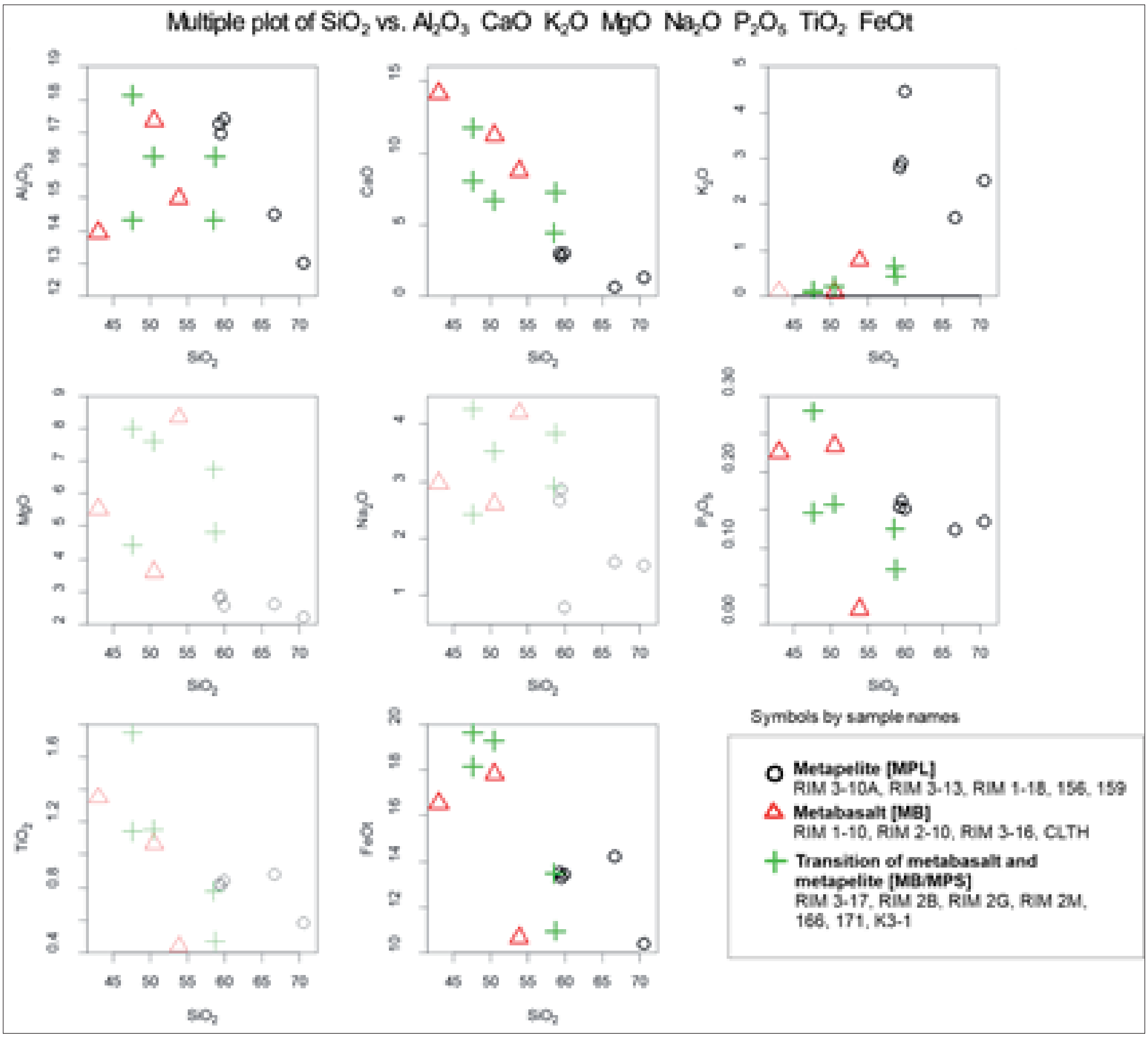

Figure 7. Correlation patterns of SiO_2 vs Major Elements. There are three main differences observed in the metapelite, metabasalt, and transitional metabasalt/metasediment samples.

Table 3. Composition of trace elements and rare earth elements in representatite samples of metamorphic rocks.

Sampel / Elemen	RIM 3-10A (MPL)	RIM 3-13 (MPL)	RIM 1-18 (MPL)	RIM 3-16 (MB)	RIM 3-17 (MB)/ (MPS)	RIM 2B (MB)/ (MPS)	RIM 1-10 (MB)	RIM 2-10 (MB)	RIM 2G (MB)/ (MPS)	RIM 2M (MB)/ (MPS)
Trace Element (ppm)										
Cd	0.15	0.18	0.12	0.15	0.06	0.3	0.53	0.55	0.15	0.21
Co	23	21	23	46	22	41	38	37	33	38
Cs	1.9	1.4	1.9	<0.1	0.2	<0.1	0.2	0.2	<0.1	0.2
Ga	25.2	21.9	21.6	18.8	17.3	18.1	14.5	13.9	16.3	15.8
Ge	1.4	1.5	1.6	1.7	1.3	1	1.2	1	1.3	1.6
Hf	0.3	0.2	0.2	0.9	0.4	1.4	0.2	0.1	1.2	0.4
In	0.11	0.14	0.1	0.13	0.08	0.1	0.07	0.09	0.07	0.09
Li	24.6	24	24.6	15	14.2	10	29.1	27.7	9.1	15.6
Mo	1.7	1.1	8.6	0.2	0.1	0.5	0.1	0.2	0.6	<0.1
Nb	9.4	9.2	9.2	1.8	0.9	16.6	1	1	10.7	2.6
Pb	18	31	7	6	6	728	18	23	2	7
Rb	131	104	92.1	0.7	7.1	0.4	5.5	5.1	0.4	6.9
Re	<0.05	<0.05	<0.05	<0.05	<0.05	<0.05	<0.05	<0.05	<0.05	<0.05
Sb	0.2	0.2	0.3	0.8	0.2	0.2	0.1	<0.1	0.1	0.4
Se	<1	<1	<1	<1	<1	<1	<1	<1	<1	<1
Sn	2.6	2.7	2.5	1.4	1.1	1.9	1.3	1.3	1.6	1.4
Sr	114	161	150	315	274	163	171	170	205	228
Ta	0.63	0.69	0.67	0.14	0.07	1.02	0.08	0.08	0.7	0.19
Te	0.3	<0.1	0.1	<0.1	<0.1	<0.1	<0.1	<0.1	<0.1	<0.1
Th	8.08	9.65	9.3	0.5	0.43	1.04	0.27	0.26	0.66	0.55
Tl	0.58	0.55	0.44	<0.02	0.04	<0.02	0.02	0.02	<0.02	0.06
U	1.58	1.4	1.72	0.27	0.1	0.32	0.13	0.15	0.21	0.19
W	1.5	0.9	1	0.1	<0.1	0.2	0.2	0.1	0.2	0.8
Y	27.2	28.6	28.2	30.5	11	28.8	22.1	21.9	19.7	27.5
Zr	8.2	4.5	4.7	20.5	8.1	38	2.5	2	30.5	6.7
REE (ppm)										
Ce	53.1	53.3	52.7	10	5.6	25.5	6.6	6.5	19.6	10.8
Dy	5.5	5.9	5.6	5.7	2.1	6.1	4.2	4.3	4.2	5.4
Er	2.9	3	2.9	3.2	1.2	3	2.4	2.4	2.4	2.8
Eu	1.5	1.5	1.5	1.4	0.6	1.8	1	1	1.1	1.3
Gd	5.5	5.9	5.9	5	1.8	5.7	3.5	3.4	4.1	4.4
Ho	1.1	1.2	1.2	1.2	0.4	1.2	0.9	0.9	1	1.1
La	23.9	25.4	23.9	5.6	2.2	11.5	2.5	2.3	8.3	3.9
Lu	0.32	0.3	0.36	0.43	0.16	0.34	0.34	0.38	0.27	0.38
Nd	26.2	27.4	26.9	11.2	4.5	16.9	6.6	6.6	13.5	9.4
Pr	6.48	6.76	6.44	2.24	0.89	3.35	1.17	1.15	2.7	1.76
Sm	5.9	6.1	5.9	3.6	1.5	5	2.5	2.4	3.7	3.4
Tb	0.88	0.94	0.9	0.85	0.33	0.95	0.62	0.62	0.66	0.8
Tm	0.4	0.4	0.4	0.4	0.2	0.4	0.3	0.4	0.3	0.4
Yb	2.7	2.6	2.6	3.2	1.2	2.6	2.4	2.4	2.2	2.6

Using the ACF triangle diagram (based on Eskola's 1939 method, modified by Winkler in 1979) and parameters like (Al_2O_3+Fe_2O_3)-(Na_2O+K_2O), FeO+MgO+MnO, and CaO, the plotted results (Figure 8-A) indicate that samples RIM 3-10A, RIM 3-13, RIM 3-16, RIM 1-18, RIM 2G, and RIM 2M fall within the Siliceous Alkali-Calsic Rocks zone, suggesting they may be greywacke or volcaniclastic rocks. Sample RIM 2B is situated in the intermediate region connecting Siliceous Alkali-Calsic Rocks and Aluminous Rocks, which could indicate the presence of clay-rich pelite. On the other hand, sample RIM-2D is categorized within the basaltic zone.

The concentrations of trace elements and Rare Earth Elements (REE) can be observed in Table 3. The concentration patterns of REEs in the samples are plotted in a normalized spider diagram relative to chondrite according to Nakamura (1974) (Figure 9-A). Based on the diagram, diverse patterns of REE distribution can be observed. Samples exhibiting metapelite characteristics [MPL] show a relatively higher concentration of Light REEs (La-Sm) that gradually decrease towards Lu. This pattern is compared to Metapelite in Manitoba, Canada (Owen, 1993), and shows a similar trend. The depletion of the Eu element is influenced by the scarcity of plagioclase in the rock. Samples with metapsammite characteristics show an enrichment towards Heavy REEs (HREE) with anomalies in Ce, which experiences depletion, and Eu, which experiences enrichment, possibly influenced by sedimentation processes and the presence of plagioclase in the source sedimentary rock. Samples with metabasalt [MB] and [MB/MPS] characteristics exhibit enrichment in HREE, suggesting the influence of oceanic plates during basalt formation.

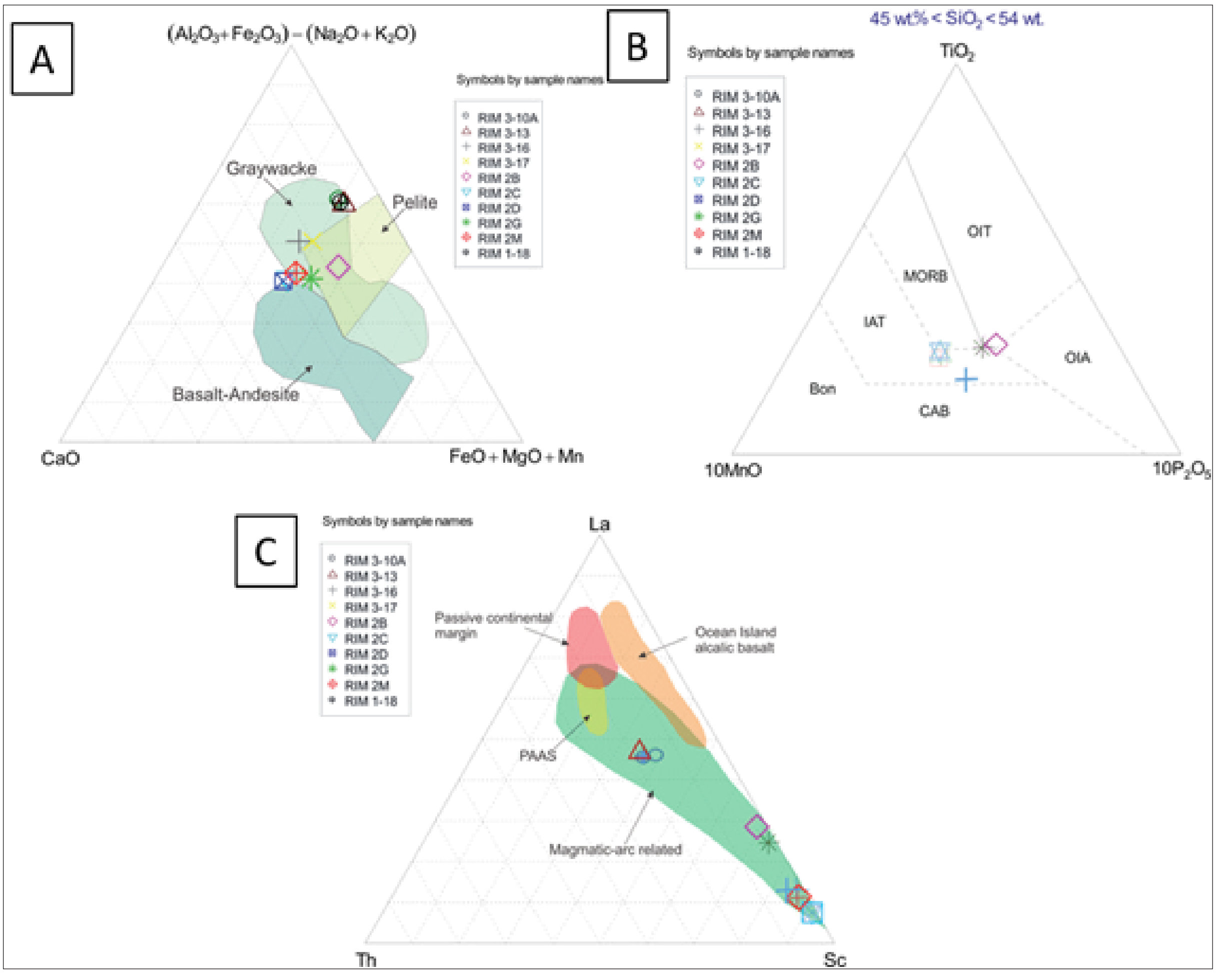

Figure 8. ACF Diagram utilized to differentiate protoliths (Winkler, 1979), (B) Concentration patterns of Rare Earth Elements (REE) and trace elements in metamorphic rocks (Mullen, 1983), (C) Identification of sediment sources in metasediments through the discrimination of La-Sc-Th (Girty and Barber,1993).

The limited presence of plagioclase in the rock explains the depletion of the Eu element. Metapsammite samples show enrichment of HREE, with specific anomalies observed in Ce and Eu. Sedimentation processes and the abundance of plagioclase in the source sedimentary rock may influence this enrichment pattern. In contrast, metabasalt samples exhibit enrichment in HREE, indicating the influence of oceanic plates during basalt formation.

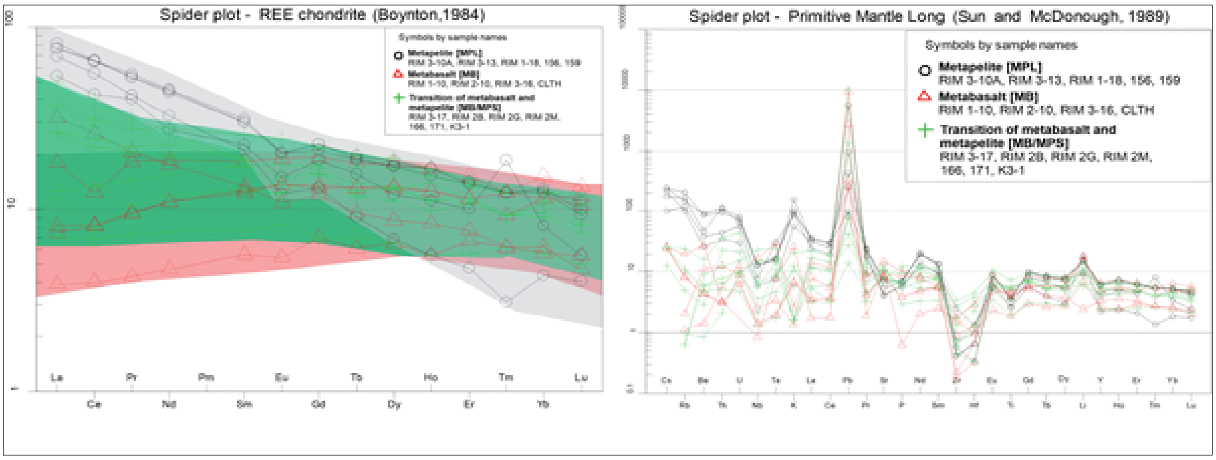

Figure 9. (A) Plotting of Rare Earth Element and Trace Element distribution in a normalized spider diagram with respect to Chondrite (Boynton, 1984) and (B) Primitive Mantle (Sun and McDonough, 1989)

The trace element concentration patterns analysis shown in Figure 9-B spider diagram reveals anomalies. Metapelite samples display an enrichment of the K element, while metabasalt samples show depletion. A consistent anomaly observed in all samples is the enrichment of the Pb element. These findings suggest possible interactions between the rocks and water, such as in subducted sedimentary rocks or hydrothermal processes. The depletion anomaly of Zr-Hf can be attributed to contamination from the continental crust during the subduction process (Zheng, 2019).

Upon analyzing the TiO_2-MnO-P_2O_5 diagram (Mullen, 1983), it is apparent that the metabasalt samples RIM 2, RIM 3-16, and RIM 17 fall within the designated field indicative of Island Arc Tholeiites. However, the remaining samples deviate from this classification due to their SiO_2 content falling below 45% or exceeding 54%. Referring to the La-Th-Sc triangle diagram following the approach outlined by Girty and Barber (1993) (Figure 8-C), it can be inferred that the sedimentary source materials in Ciletuh originate from an environment associated with a magmatic arc.

K-Ar Dating of Metamorphic Rocks

The absolute age of metamorphic rocks was determined using the K-Ar method. The results indicate that the age of the metamorphic rocks ranges from 55.2 to 37.8 million years ago, corresponding to the Early Eocene to Late Eocene period (refer to Table 4). This age is significantly younger than the previous estimates, which suggested a Cretaceous age or an age older than 65 million years. However, these findings cannot be considered a definitive reference for the age of the metamorphic rocks due to the analysis being conducted on bulk samples.

Table 4. Ages of Metamorphic Rocks based on radiometric K-Ar dating

Sample No	Rock Name	Age (Ma)	Error 2 Σ	Geological Age	Analitical Method
RIM 1-5 (156)	Muscovite-Chlorite-Epidote Schist	**55,2**	**2**	Yppresian –Early Eocene	*Bulk Sample*
RIM 1-12 (171)	Muscovite-Chlorite-Epidote Schist	**37,8**	**1,5**	Priabonian-Late Eocene	*Bulk Sample*
RIM 3-13 (159B)	Chlorite-Muscovite-Graphite Schist	**54,7**	**1,4**	Yppresian – Early Eocene	*Bulk Sample*

This limitation of this bulk sample K-Ar dating arises from the mineralogical processes within metamorphic rocks that often undergo multiple recrystallization events, leading to potential biases in determining the age of mineral formation. The reported age figures may represent the age of the protolith before metamorphism, the age of metamorphic formation, or the age of retrograde metamorphism during uplift. This paper provides age information is as a temporary representation, indicating a recorded time interval during several phases of metamorphism.

Metamorphic Process and Its Implication in Paleo-Tectonic Reconstruction

The protolith of metamorphic rocks in Ciletuh indicates the origin of both oceanic and continental crustal components. This suggests that the formation environment of the metamorphic rocks occurred at the convergence of these two crustal types. However, based on the formed facies, the metamorphism was not caused by deep subduction, which would result in ultrahigh-pressure or ultrahigh-pressure-temperature metamorphism. The TiO_2-MnO-P_2O_5 diagram, used for tectonic discrimination, reveals that the metabasites formed within an Island Arc environment. This suggests the occurrence of tectonic interactions between two oceanic crusts, where one plate undergoes subduction beneath the other. The unidentified oceanic crust is positioned at the outer boundary of the continental plate, known as the Supra-Subduction Zone (SSZ).

Local magmatism and island arcs is a direct consequence of the subduction process, as evident from the alteration characteristics observed in metamorphic rocks. In some instances, mineralization processes take place, indicated by the presence of iron sulfides. Furthermore, local magmatism contributes to elevated metamorphic temperatures, leading to the development of amphibolite facies.

This interpretation has sparked debates regarding the involvement of specific oceanic plates in the subduction process. However, several studies suggest the possibility of similar tectonic settings in other regions, such as the Meratus Tectonic Belt in Kalimantan (Wakita, 1999) and the southern part of Sumatra (Zulkarnain, 2011), as illustrated in Figure 10.

Previously, it has been elucidated that the age of metamorphic rocks in Ciletuh falls 55.2 - 37.8 million years ago, equivalent to the Early to Late Eocene period. Meanwhile, the age of gabbro in Ciletuh is determined to be 56.0 ± 2.3 million years ago and 50.9 ± 2.1 million years ago (Schiller, 1998), indicating the formation of ophiolite during the Early Eocene. It is hypothesized that the ophiolite formation occurred in an Island Arc environment (Patonah and Permana, 2010; Patonah, 2011; Ikhram, 2019). Temporarily, the metamorphism is believed to have occurred concurrently with or after the ophiolite formation.

The metamorphic rocks discovered in the Cikopo River display retrogradation characteristics, where the metamorphic grade undergoes a transition from medium-grade amphibolite and epidote amphibolite to lower-grade greenschist. The greenschist exhibits either albite-tremolite-actinolite-chlorite or talc-chlorite mineral assemblages. These two groups of amphibolite schists originate from basaltic rocks that have undergone compositional changes at temperatures ranging from approximately 500°-600°C and pressures of about 5-6 kbar (Butcher and Rodney, 2011).

As mentioned, the formation of lower-grade metamorphic rocks, as mentioned, is likely attributed to a retrograde metamorphism (temperatures around 300°-400°C and pressures below 4 kbar). Deformation data observed in both the Citisuk and Cikopo Rivers indicate a relative movement of the basement blocks from north to south or northwest to southeast. The microstructures formed by secondary minerals such as chlorite or actinolite along the structural planes suggest that these structures formed at low temperatures, with their directional characteristics interpreted as a result of rock shearing within an accretion system (Ikhram, 2019).

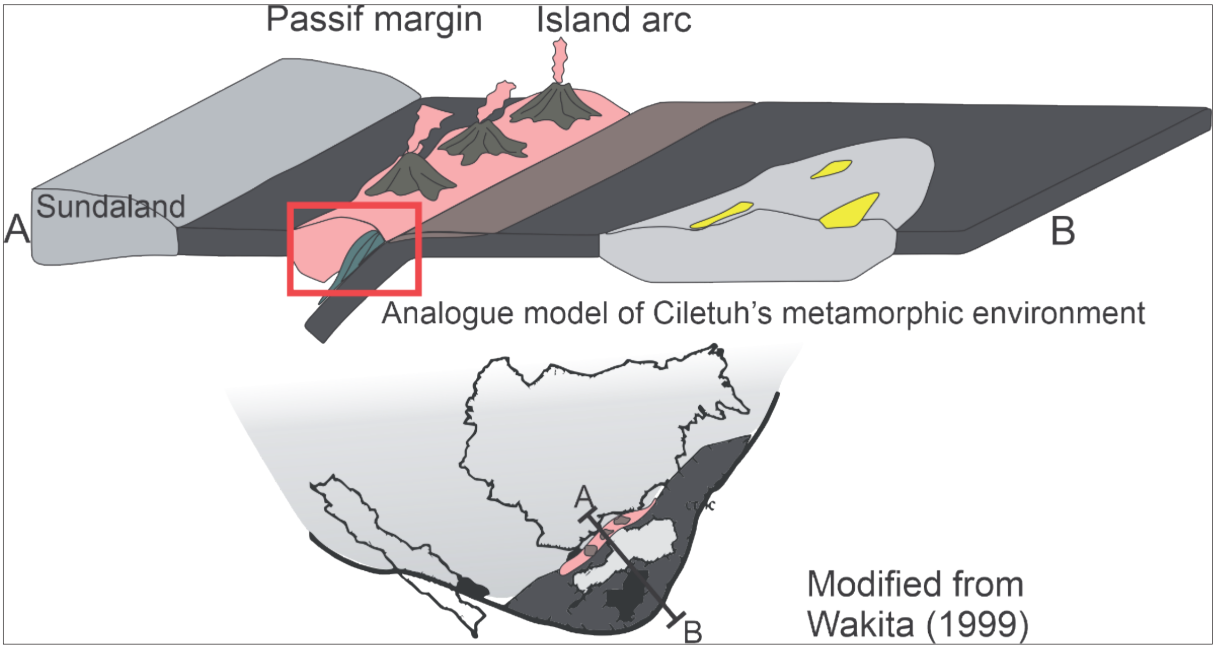

Figure 10. Modified Cartoon of the Tectonic Mechanism in the Meratus Region, Kalimantan (Wakita, 1999), as an adopted model demonstrating the existence of a paleo-island arc in Ciletuh.

This metamorphic process is interpreted to have occurred in a relatively shallow subduction zone. However, the period of subduction that led to this metamorphism has yet to be confirmed. Considering the age determination based on K-Ar dating, the subduction and accretion processes likely occurred during the early Eocene period (around 55-54 Ma) until the late Eocene (approximately 37 Ma).

Subsequently, these metamorphic rocks underwent accretion simultaneously with the emplacement of oceanic crustal rocks derived from the volcanic arc basement that formed during the Eocene period. Along with this accretion process, sedimentary deposits that comprise the Ciletuh Formation were also deposited. This argument is further supported by the embedded mudstone fragments within the schists in the Citisuk River.

CONCLUSION

The dominant composition of the metamorphic rocks within the Ciletuh mélange complex consists of greenschist facies rocks, and retrograde amphibolites. These rocks originate from various protoliths, including mudstone, sandstone, carbonate sandstone, and basalt. This suggests the existence of a rock unit that formed in a marine environment, accompanied by submarine volcanism, during the pre-Eocene period, specifically the Cretaceous to Paleocene era.

During the early Eocene period, these rock units underwent metamorphism due to shallow subduction, resulting in low to moderate metamorphic grades. This subduction also gave rise to an island arc, as evidenced by the presence of ophiolites in the Ciletuh region. The metamorphic rocks and ophiolites subsequently accreted within an accretionary prism, forming the mélange.

ACKNOWLEDGMENTS

The author acknowledges the support provided by the Academic Leadership Grant (ALG) from the Directorate of Research, Community Service, and Innovation of Universitas Padjadjaran. This grant has played a crucial role in supporting research activities of the Ciletuh-Palabuhanratu Geopark, for which the author is grateful. The K-Ar dating process was carried out with funding support from PT. Pertamina and served as part of collaborative research with Universitas Padjadjaran.

REFERENCE

Butcher K., dan Rodney. G., 2011. Petrogenesis of Metamorphic Rocks, 8th ed. Springer Heidelberg Dordrecht, London, New York.Boynton, W.V., 1984. Cosmochemistry of the rare earth elements: meteorite studies. In Developments in geochemistry (Vol. 2, pp. 63-114). Elsevier.

Dirk, M. H. J., 1997, Studi petrologi batuan ofiolit dari kompleks bancuh Ciletuh, Jawa Barat, JurnalGeologi dan Sumberdaya Mineral, v. VII, p. 26-31.

Girty, G. H. and Barber, R. W., 1993. REE, Th, and Sc evidence for the depositional setting and source rock characteristics of the Quartz Hill chert, Sierra Nevada California. Processes Controlling the Composition of Clastic Sediments Geol. Soc. Amer. Spec. Pap. 284, 109–119

Ikhram., R., et., al., 2019. Petrological Characteristic and Whole Rock Geochemistry of Metamorphic Rocks in Melangè Complex of Ciletuh Area, West Java, Indonesia. International Journal on Advanced Science, Engineering and Information Technology (IJASEIT). Vol 9, No 6.

Mullen, E. D., 1983. $MnO/TiO_2/P_2O_5$: a minor element discriminant for basaltic rocks of oceanic environments and its implications for petrogenesis. Earth and Planetary Science Letters 62, 53–62.

Nakamura, N., 1974. Determination REE, Fe, Mg, Na, and K in carbonaceous and ordinary chondrites. Geochim. Cosmochim. Acta, 32, 757-775. (2002)

Owen, J. V. et, al., 1993. Mineralogic reaction zones at a calc-silicate/metapelite interface: an example of trace element mobility in a metamorphic environtment. Mineralogical Magazine, June 1994, Vol. 58, pp. 205-214

Patonah, A. and Permana, H., 2010. Petrologi amfibolit komplek melange Ciletuh, Jawa Barat. Bul. Sci. Contrib, 8, pp.69-77.

Patonah, A., 2011. Lingkungan Tektonik Ofiolit Komplek Melange Ciletuh Jawa Barat Berdasarkan pendekatan Petrologi. Bul. Sci. Contrib, Vol. 9, No. 3, pp. 139-151

Prasetyo, A., et.al., 2016, A petrological review of metamorphic rocks from Ciletuh complex, in West Java and their related metamorphism in Central Indonesia region, Proceedings Seminar Nasional Kebumian ke-9, 6-7 October 2016, Yogyakarta

Thayyib E. S., dkk., 1977, The status of the mélange complex in Ciletuh area, Southwest Java: Proceeding Indonesia Petroleum Assoc., 6th annual conv., hal 241-253.

Sartono, S., dan Murwanto, H., 1987, Olitostrom sebagai batuan dasar di Jawa, Proceeding PIT XVI IAGI, 19 pages.Suparka, M.E.R., 1995, Studi Komplek Ofiolit Ciletuh, Jawa Barat (Pola Sebaran, Macam Batuan, Petrologi, serta Pola Kimia), InstitutTeknologi Bandung, unpublished

Schiller, D.M., Garrard, R.A., Prasetyo Ludi, 1991. Eocene Submarine fan sedimentation in Southwest Java. Proceedings IPA ke 20, Jakarta.

Sukamto, Rab, 1975: Geologi Lembar Jampang dan Balekambang, Skala 1:100.000. Direktorat Geologi Bandung

Sun S.S. dan McDonough W. F., 1989, Chemical and isotopic systematics of oceanic basalts: implication for mantle compotition and processes. Geol Soc. London. Spec. Pub. 42, pp. 313-345.

Wakita K, Miyazaki K, Zulkarnain I, Sopaheluwakan J, and Sanyoto P, (1998): Tectonic implications of new age data for the Meratus Complex of South Kalimantan, Indonesia, The Island Arc, 7, pp 202-222.

Winkler, H. G. F., 1976. Petrogenesis of Metamorphic Rocks. 4th ed. Springer-Verlag, New York. 334

Zheng, Y.F., 2019. Subduction zone geochemistry. Geoscience Frontiers, 10(4), pp.1223-1254.

Zulkarnain, I., 2011. Geochemical evidence of island-arc origin for Sumatra Island; a new perspective based on volcanic rocks in Lampung Province, Indonesia. Indonesian Journal on Geoscience, 6(4), pp.213-225.